Journal of Neurochemistry

JOURNAL OF NEUROCHEMISTRY | 2010 | 114 | 784–794 doi: 10.1111/j.1471-4159.2010.06812.x

Characterization of AZD4694, a novel fluorinated Aβ plaque neuroimaging PET radioligand

Anders Juréus,* Britt-Marie Swahn,† Johan Sandell,† Fredrik Jeppsson,* Allan E. Johnson,*,[1] Peter Johnström,† Jan A. M. Neelissen,‡ Dan Sunnemark,* Lars Farde§,¶ and Samuel P. S. Svensson*

*Department of Neuroscience, AstraZeneca R&D Södertälje, Södertälje, Sweden

†Medicinal Chemistry, AstraZeneca R&D Södertälje, Södertälje, Sweden

‡DMPK, AstraZeneca R&D Södertälje, Södertälje, Sweden

§Discovery Medicine, AstraZeneca R&D Södertälje, Södertälje, Sweden

¶Department of Clinical Neuroscience, PET Centre, Karolinska Institutet, Karolinska University Hospital, Stockholm, Sweden

Abstract

Positron emission tomography (PET) radioligands that bind selectively to β-amyloid plaques (Aβ) are promising imaging tools aimed at supporting the diagnosis of Alzheimer's disease and the evaluation of new drugs aiming to modify amyloid plaque load. For extended clinical use, there is a particular need for PET tracers labeled with fluorine-18, a radionuclide with 110 min half-life allowing for central synthesis followed by wide distribution. The development of fluorinated radioligands is, however, challenging because of the lipophilic nature of aromatic fluorine, rendering fluorinated ligands more prone to have high non-specific white matter binding. We have here developed the new benzofuran-derived radioligand containing fluorine, AZD4694 that shows high affinity for β-amyloid fibrils *in vitro* (K_d = 2.3 ± 0.3 nM). In cortical sections from human Alzheimer's disease brain [^{3}H]AZD4694 selectively labeled β-amyloid deposits in gray matter, whereas there was a lower level of non-displaceable binding in plaque devoid white matter. Administration of unlabeled AZD4694 to rat showed that it has a pharmacokinetic profile consistent with good PET radioligands, i.e., it quickly entered and rapidly cleared from normal rat brain tissue. *Ex vivo* binding data in aged Tg2576 mice after intravenous administration of [^{3}H]AZD4694 showed selective binding to β-amyloid deposits in a reversible manner. In Tg2576 mice, plaque bound [^{3}H]AZD4694 could still be detected 80 min after i.v. administration. Taken together, the preclinical profile of AZD4694 suggests that fluorine-18 labeled AZD4694 may have potential for PET-visualization of cerebral β-amyloid deposits in the living human brain.

Keywords: Alzheimer's disease, amyloid, neuroimaging, positron emission tomography, Tg2576.

J. Neurochem. (2010) **114**, 784–794.

Accurate diagnosis of Alzheimer's disease (AD) can presently only be obtained postmortem by confirming histopathological presence of extracellular Aβ plaques (diffuse, fibrillar, and vascular plaques) and neurofibrillary tangles (NFT), the two hallmarks of the disease (Braak and Braak 1991). The precise pathological role of Aβ plaques in AD is not yet clear mainly because of the lack of correlation between cognitive decline and levels of plaques (Nelson *et al.* 2009). Evidence suggests a causative relationship between Aβ plaques and NFT's, where Aβ plaques gradually accumulate, stimulating NFT formation, and subsequent neurodegeneration (Bennett *et al.* 2004; Nelson *et al.* 2009).

Interestingly, postmortem analysis and positron emission tomography (PET) neuroimaging studies have shown that a large proportion (20–40%) of non-demented elderly has a substantial amount of Aβ plaques (Price *et al.* 1991; Knopman *et al.* 2003; Aizenstein *et al.* 2008; Villemagne *et al.* 2008). A recent study suggests that although this group has previously been considered to be non-demented and without symptoms,

Received February 4, 2010; revised manuscript received April 30, 2010; accepted April 30, 2010.

Address correspondence and reprint requests to Samuel Svensson, Ph.D., Department of Neuroscience, Local Discovery Research Area CNS & Pain control, AstraZeneca R&D Södertälje, SE-15185 Södertälje, Sweden. E-mail: samuel.svensson@astrazeneca.com

[1]In memory of Allan E. Johnson.

Abbreviations used: AD, Alzheimer's disease; ApoE, apolipoprotein E; Aβ, β-amyloid; DMSO, dimethylsulfoxide; IHC, immunohistochemistry; NFT, neurofibrillary tangles; PET, positron emission tomography; PI, phosphorimage; PIB, Pittsburgh investigating compound B; S/N, signal-to-noise.

the presence of Aβ plaques in fact appear to be associated with minor cognitive dysfunction, aberrant functional magnetic resonance imaging patterns, but without substantial neurodegeneration (Price *et al.* 2009; Sperling *et al.* 2009). The presence of Aβ plaques, with very minor cognitive dysfunction may thus indicate a prodromal stage of AD where emerging disease-modifying therapies would have a greater possibility to achieve a preventive and more durable beneficial effect (Pike *et al.* 2007 Morris *et al.* 2009).

Positron emission tomography neuroimaging of Aβ plaques with radioligands such as the thioflavin derivatives [^{11}C]Pittsburgh investigating compound B (PIB), [^{18}F]flutemetamol (fluorine-18 labeled F-PIB) stilbene derivatives [^{18}F]florbetaben ([^{18}F]BAY94-9172), and [^{18}F]florpiramine ([^{18}F]AV45) are promising tools that might support and increase specificity when diagnosing preclinical AD (Klunk *et al.* 2004; Mathis *et al.* 2007a; Rowe *et al.* 2008). PET neuroimaging of cerebral Aβ plaques might also be useful for the evaluation of new therapies aiming to modify plaque load and for patient stratification in clinical trials (Mathis *et al.* 2007b; Rinne *et al.* 2010).

None of the fluorine-18 labeled Aβ plaque-selective PET tracers currently in clinical development, flutemetamol, florbetaben, and florpiramine has been evaluated side-by-side *in vitro* or *in vivo.* Consequently, a true comparison is lacking. Another approach would be to compare preclinical and clinical data with [^{11}C]PIB, the most widely used Aβ plaque-selective PET radioligand. This approach has been suggested by Klunk and Mathis (2008), and applied for flumetamol (Mathis *et al.* 2007a). Despite the lack of direct comparisons, it is clear that the Aβ plaque-selective fluorine-18 labeled PET radioligands flutemetamol, florbetaben, and florpiramine all show high levels of non-specific white matter retention, most likely more than [^{11}C]PIB. The mechanism of white matter retention seems to be owing to non-saturable non-specific binding that to some degree is governed by the lipophilicity (LogD) of the compound (Fodero-Tavoletti *et al.* 2009; Johnson *et al.* 2009). High non-specific white matter retention may limit the sensitivity of PET imaging especially in a prodromal phase of AD when plaque levels might be low.

We recently developed an Aβ plaque-selective carbon-11 labeled PET radioligand named [^{11}C]AZD2184, which has the positive attributes of [^{11}C]PIB but with an apparent lower degree of non-specific binding (Johnson *et al.* 2009; Nyberg *et al.* 2009). The short half-life of carbon-11 (20 min), however, limits its potential as a widely used clinical diagnostic tool. A radioligand labeled with the longer lived radionuclide fluorine-18 (110 min) would be more useful for this purpose since it could be regionally distributed to PET imaging centers that lack in house cyclotron and radiolabeling facilities.

The aim with this study was to develop a selective and sensitive fluorine-18 labeled PET radioligand of cerebral fibrillar Aβ-amyloid with a low level of non-specific white matter binding. This article describes *in vitro* as well as *in vivo* characterization of a fluorinated candidate ligand named AZD4694. The study includes a side-by-side comparison between AZD4694, PIB, and flutemetamol binding to synthetic Aβ fibrils and autoradiography in brain tissue from transgenic mice (Tg2576) and AD patients.

Materials and methods

Preparation of Aβ(1–40) and Aβ(1–42) fibrils

Fibril stock solutions were prepared by dissolving Aβ(1–40) peptides (Bachem, Torrance, CA, USA) in 100 mM NaOH to a concentration of 2 mg/mL followed by water bath sonication for 30 s. The stock solutions were then further diluted to 100 μM in 10 mM HEPES, 100 mM NaCl, and 0.02% sodium azide at pH 7.4, and incubated with slow magnetic stirring at 22°C for 6 days before being frozen in aliquots at −80°C (Necula *et al.* 2007). The formation of fibrils was confirmed with Thioflavin-T fluorescence (Nilsson 2004) and atomic force microscopy (data not shown).

Fibril stock solutions of Aβ(1–42) were prepared by dissolving peptides (Bachem) in dimethylsulfoxide (DMSO) followed by vortexing and further dilution to 100 μM in phosphate-buffered saline. The solution was incubated with slow magnetic stirring at 22°C for 4 days before being frozen in aliquots at −80°C (Yang *et al.* 2005).

Experimental animals

Female APP_{SWE} transgenic mice (Tg2576) mice, 12–24 months old, weighing 17–25 g (Taconic, Ejby, Denmark) were used for *in vitro* and *ex vivo* autoradiography experiments.

Male Sprague–Dawley rats (275–300 g; Scanbur B&K AB, Sollentuna, Sweden) were used to measure plasma and brain exposure after *in vivo* drug administration. All animals were housed at the AstraZeneca animal facility (AstraZeneca R&D, Södertälje, Sweden). Housing was humidity and temperature controlled. Food and water was provided *ad libitum* and the light/dark cycle was 12/12 h. All animal studies were approved by the Stockholm Animal Research Ethical Committee and all experiments were performed in accordance with guidelines from the Swedish Animal Welfare Agency.

Human tissue

Cortical samples from AD patients were acquired from the Netherlands Brain Bank and used to examine the binding of test compounds to β-amyloid plaques. The tissue samples were used in accordance with the Swedish Biobank Law and AstraZeneca guidelines to protect the integrity of the donor. Cortical samples from a female, 94 years old, Braak stage 4, apolipoprotein E (ApoE) type 4/3, inferior frontal gyrus; female, 67 years old, Braak stage 6, ApoE type 3/3, inferior frontal gyrus; female, 89 years old, Braak stage 5, ApoE type 4/3, inferior frontal gyrus were used.

Tritium labeling of AZD4694, flutemetamol and PIB

[^{3}H]AZD4694 was synthesized by alkylation of 6-fluoro-5-(5-methoxy-1-benzofuran-2-yl)pyridin-2-amine with [3H]methyl

iodide in dimethylformamide as solvent and sodium hydride as base. After purification on C8 reversed phase HPLC the methoxy group was demethylated with boron tribromide in dichloromethane as solvent. Subsequently, [3H]AZD4694 was purified on C8 reversed phase HPLC. [^{3}H]Flutemetamol was synthesized in an analogous way. [3H]PIB was prepared following a previously published method (Klunk *et al.* 2004). [^{3}H]AZD4694, [^{3}H]Flutemetamol, and [^{3}H]PIB were stored in absolute ethanol at −18°C and the specific activities were 2.8 TBq/mmol. The radioactive purity was in all cases > 98%.

ElogD measurement

LogD values were measured (ElogD) as previously described (Lombardo *et al.* 2001).

Radioligand binding assay

Saturation binding assays on human Aβ(1–40) fibrils were performed to determine the equilibrium dissociation constant (K_d) as has been previously described (Johnson *et al.* 2009). Briefly, 0.20 μM synthetic human Aβ(1–40) fibrils in phosphate buffer (pH 7.5) were incubated with increasing concentrations of [^{3}H]AZD4694 or [^{3}H]flutemetamol for 3 h at 22°C. Non-specific, non-displaceable binding was defined in the presence of 50 μM Thioflavin-T diluted in DMSO (final concentration 0.5%). The incubation was terminated by filtration through Whatman GF/B glass filter (Whatman International, Kent, UK), and washed rapidly three times with 2 mL of ice-cold wash buffer (10 mM HEPES pH 7.4 containing 500 mM NaCl). The filters were equilibrated for 2 h in scintillation vials containing 4 mL of Ultima Gold scintillation fluid before counted in a Packard Tricarb 2900TR Liquid Scintillation Analyzer (PerkinElmer, Waltham, MA, USA). All data points were performed in duplicate and repeated at least three times. The binding data were evaluated by fitting the data to a one-site binding model using GraphPad Prism, version 4.03 (GraphPad Software, San Diego CA, USA).

AZD4694 competition at [^{3}H]AZD2184 binding was examined in 384-well Multiscreen HTS FB plates coated with 50 μL 2% bovine serum albumin in phosphate buffer pH 7.5 (Johnson *et al.* 2009). The reaction mixtures consisted of 2 μM of Aβ(1–40) or Aβ(1–42) fibrils in phosphate buffer (pH 7.5), test compound diluted in DMSO or DMSO alone (2% final concentration of DMSO), and 3 nM [^{3}H]AZD2184 diluted in phosphate buffer pH 7.5 containing 0.1% bovine serum albumin. The reaction mixture was incubated for 30 min at 22°C and terminated by vacuum filtration followed by two consecutive washes with 80 μL of ice-cold buffer (10 mM HEPES pH 7.4 containing 500 mM NaCl, 1% Triton-X100). After drying, Ultima Gold scintillation fluid was added to each well and the plates were sealed and equilibrated for 1 h at 22°C before being read in a Wallac Microbeta 1450 plate reader (PerkinElmer, Waltham, MA, USA). Non-specific binding was defined as the number of counts from wells containing reaction mixtures lacking Aβ fibrils. The K_i-values for AZD4694 and flutemetamol competition at [^{3}H]AZD2184 binding were determined by fitting the data to one-site competition model using GraphPad Prism, version 4.03 (GraphPad Software). All measurements were performed in duplicate and each experiment was repeated at least four times. Means of K_d, B_{max}, and K_i were compared by *t*-test using GraphPad Prism, version 4.03 (GraphPad Software). Differences were considered significant at $p < 0.05$.

In vitro autoradiography on brain sections from AD patients

In vitro autoradiography was performed as has been described earlier (Johnson *et al.* 2009). Briefly, 10 μm thick cry-cut tissue sections from Tg2576 or human postmortem AD brain thaw-mounted onto microscope slides (SuperFrost® Plus slides; Menzel GmbH, Braunschweig, Germany) were incubated in 50 mM Tris buffer (pH 7.4) at 22°C followed by 30 min incubation with 1, 3, or 10 nM of [^{3}H]AZD4694 or [^{3}H]flutemetamol in Tris buffer. For competition studies *in situ*, cortical brain sections from AD patients were first pre-incubated for 30 min at 22°C in 50 mM Tris buffer (pH 7.4) with competing PIB then incubated for 30 min at 22°C in 50 mM Tris buffer (pH 7.4) together with 1 nM [^{3}H]AZD2184 in the presence of increasing concentrations of PIB. Finally, the sections were washed (3 × 10 min) in Tris buffer (1°C) followed by a rinse in deionized water (1°C) and air-dried at 22°C in front of a fan.

Radiolabeled sections and plastic tritium standards (Amersham Pharmacia Biotech, Piscataway, NJ, USA) were exposed to phosphorimage (PI) plates (Fuji BAS-TR2040) overnight. Phosphorimage plates were processed with a Fujifilm FLA7000 phosphorimager (Fuji, Tokyo, Japan). Binding was analyzed with Multigauge software V3.0 (Fuji) using the relative optical density values generated from co-exposed tritium standards to calculate binding values in mol/mg. To determine signal-to-noise (S/N) ratio, the region of interest in gray and white matter (prefrontal cortex, AD) was outlined with Multi Gauge V3.0 software (Fuji) and the optical densities measured as digital light units per square millimeter. S/N was obtained by taking total binding (gray matter regions) minus non-specific binding (subcortical white matter region) and then divided by non-specific binding (subcortical white matter region) (i.e., specific binding/nonspecific binding).

Binding curves and K_i-values were generated with GraphPad Prism, version 4.03 (GraphPad Software).

High-resolution autoradiography

Emulsion dipped [^{3}H]AZD4694 labeled tissue sections for microscope analysis were prepared as described earlier (Johnson *et al.* 2009). In short, 10 μm slide-mounted cryo-cut tissue sections were labeled with 1 nM of [^{3}H]AZD4694 and dipped in NTB-2 liquid emulsion (Kodak, Rochester, NY, USA) at 42°C. The slides were air-dried and exposed for 1–2 weeks in the dark, developed, and counter-stained with hemotoxylin (Histolab, Göteborg, Sweden). Finally they were cover-slipped with Kaiser's glycerol gelatin (Merck, Darmstadt, Germany).

Aβ plaque immunohistochemistry

Frozen tissue sections from Tg2576 mouse brain and AD cortex were fixed by immersion in 50% acetone for 1 min and 100% acetone for 7 min. The immunohistochemical procedure was carried out on an automated stainer (Ventana Discovery® XT staining module, Ventana, Illkirch, France) using Ventana kits and the manufacturer's prescribed 'no pre-treatment' protocol. A mix of two different primary antibodies, 4G8 (Signet, Dedham, MA) detecting β-amyloid (27–24) and 6E10 (Signet, Dedham, MA, USA) β-amyloid (1–16), was manually applied at a 1 : 1000 dilution (1 μg/mL) for detection of total plaque load.

The Ventana Omni-ultramap kit was used for detection. Finally, the slides were counter-stained with hematoxylin and analyzed under light microscope.

Brain exposure

Intravenous cassette dosing with flutemetamol and AZD4694 was used to compare the *in vivo* pharmacokinetic characteristics as has been described earlier (Johnson *et al.* 2009). Compounds were dissolved in a polyethylene glycol 400 : dimethylamide : water mixture (40 : 40 : 20 v/v/v) at a concentration of 0.25 μmol/mL each, and administered to rats (slow bolus dose, 4 mL/kg, three rats per time point). Prior to decapitation, blood samples (400 μL) were collected from the tail vein 2 and 30 min after dosing, immediately placed on ice, and centrifuged within 30 min at 4°C for 5 min at 2000 *g* to obtain plasma. Brains were removed, homogenized in cold (4°C) Ringer solution (1 part brain + 2 parts Ringer, w/v, ULTRA-Turrax T8 homogenizer; IKA, Staufen, Germany), and sonicated (Ultrasonic Processor UP200H; Hielscher Ultrasonics, Berlin, Germany). Plasma and brain samples were precipitated with acetonitrile and after mixing and centrifugation, the supernatant was diluted with mobile phase and analyzed by liquid chromatography coupled with tandem mass spectrometry.

Ex vivo autoradiography

The *in vivo* binding of [^{3}H]AZD4694 to Aβ plaques in Tg2576 mice was performed as described in (Johnson *et al.* 2009). Naïve, awake Tg2576 mice were intravenously infused via the tail vein over a 30 s period with [^{3}H]AZD4694 (150 nmol/kg). The mice were rapidly anesthetized with isofluorane and decapitated at different time points after drug administration.

For comparison with [^{3}H]flutemetamol, animals (n = 2) were killed 10 min after compound administration. To obtain a curve for [^{3}H]AZD4694 plaque binding versus time, animals (n = 2) were killed 5, 15, 40, and 80 min after drug administration.

Brains were processed as described earlier (Johnson *et al.* 2009). Rinsed and unrinsed sections together with tritium standards were exposed overnight to PI plates (Fuji BAS-TR2040).

To determine signal/noise ratio, regions of interest in gray (plaques) and white matter (corpus callosum) were outlined with Multi Gauge V3.0 software (Fuji) and the optical densities measured as digital light units per square millimeter. The signal obtained over plaques was then divided by the signal obtained in the white matter region (non-specific binding, Figure 5). To analyze the plaque labeling with time after [^{3}H]AZD4694 *in vivo* administration, plaque area fraction analysis was performed with the NIH-ImageJ V14.0 software (National Institute of Mental Health, Bethesda, MD, USA). Data are expressed as area fraction of the number of pixels corresponding to labeled amyloid plaque divided by the total area of the brain in pixels.

Selectivity screen

The selectivity of AZD4694 was evaluated in a profiling screen against a panel of 99 enzymes, receptors, transporters, and ion channels. AZD4694 was tested at a single concentration of 10 μM (MDS Pharma Service, Taipei, Taiwan).

Results

Radioligand binding

The benzofuran series was identified in an effort to find new chemical scaffolds suitable for fluorine-18 radiolabeling. The compound named AZD4694 with fluorine in position 2′ displayed highest affinity in our screening assay (Fig. 1). AZD4694 was able to fully compete with 3 nM [^{3}H]AZD2184 binding to synthetic Aβ(1–40) fibrils (Fig. 2a) as was flutemetamol. The resulting K_i-values for AZD4694 (18.5 ± 2.4 nM, n = 4) and flutemetamol (15.3 ± 2.4 nM, n = 5) were not significantly different (p = 0.37). The K_i-values were calculated using the previously reported K_d-value for AZD2184 (8.4 ± 1 nM) (Johnson *et al.* 2009). The values were not significantly different (p = 0.37). AZD4694 binding to Aβ(1–42) fibrils was evaluated in a similar competition assay using [^{3}H]AZD2184. The results were not significantly different compared to Aβ(1–40) fibrils.

To quantify the degree of non-specific and specific binding, AZD4694 and flutemetamol were labeled with tritium and the binding characteristics *in vitro* to Aβ(1–40) fibrils and brain tissue slices were determined. Saturation binding studies with up to 11 nM of [^{3}H]-ligand showed that [^{3}H]AZD4694 bound with high affinity to Aβ(1–40) (Table 1) fibrils (K_d = 2.3 ± 0.3 nM, with a B_{max} of 1.7 ± 0.4 pmol/nmol Aβ(1–40); Fig. 2b). The corresponding

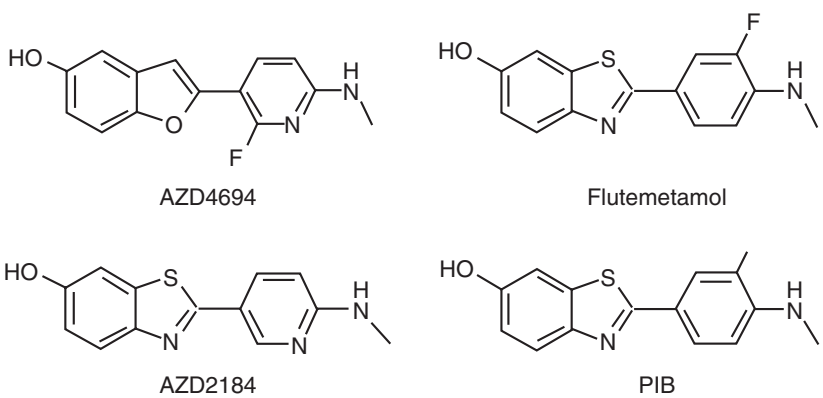

Fig. 1 Structure of AZD4694 (WO2008/108730), flutemetamol, AZD2184, and PIB.

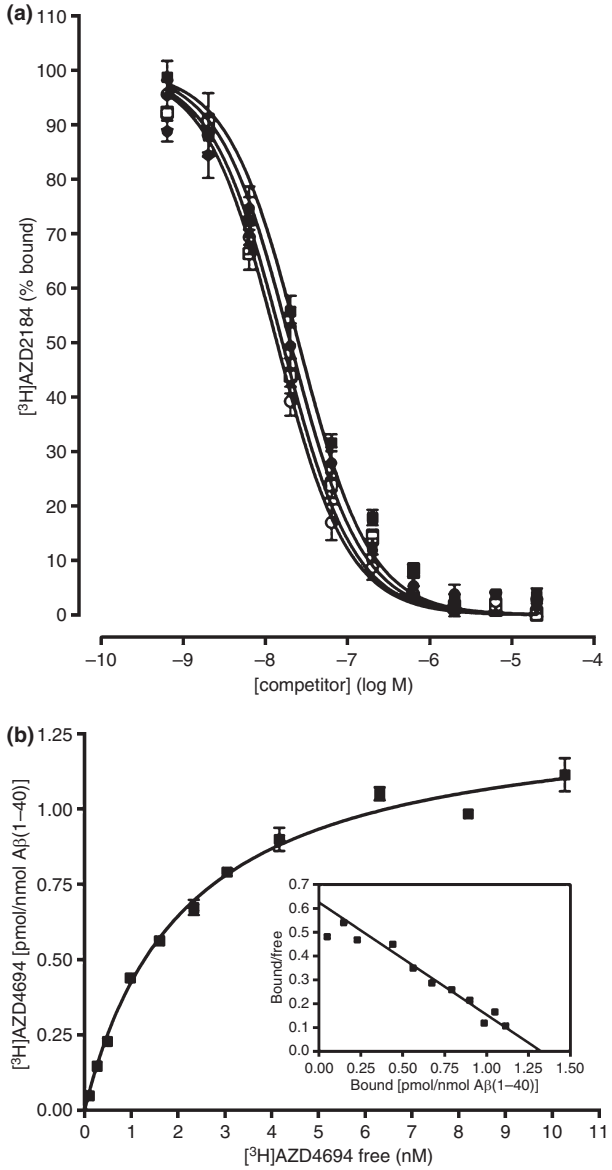

Fig. 2 (a) Displacement of 3 nM [^{3}H]AZD2184 binding from synthetic human Aβ(1–40) fibrils by increasing concentrations of AZD4694 (■), AZD2184 (□), flutemetamol (●), and PIB (○). The graph shows the mean of at least eight data points ± SEM. (b) Saturation binding of [^{3}H]AZD4694 to synthetic human Aβ(1–40) fibrils. Representative graph showing duplicate data points ± range.

dissociation constant (K_d) for [^{3}H]flutemetamol was found to be 1.6 ± 0.2 nM, and the B_{max} was 0.8 ± 0.1 pmol/nmol Aβ(1–40). The estimated ElogD for AZD4694 and flutemetamol were 2.8 and 3.2, respectively.

The specificity of AZD4694 binding was also examined through competition of [^{3}H]AZD2184 binding in postmortem brain sections from AD patients. AZD4694 inhibited [^{3}H]AZD2184 binding (1 nM) in a concentration-dependent manner, with a K_i of 23.1 nM (Fig. 3c).

Table 1 Binding affinity (K_d) and capacity (B_{max}) of [^{3}H]AZD4694 and [^{3}H]flutemetamol to synthetic human Aβ(1–40) fibrils *in vitro*

	K_d (nM; mean ± SEM)[a]	B_{max} (pmol/nmol Aβ; mean ± SEM)[b]
AZD4694 (n = 5)	2.3 ± 0.3	1.7 ± 0.4
Flutemetamol (n = 3)	1.6 ± 0.2	0.8 ± 0.1

[a]The binding affinity of [^{3}H]AZD4694 was not significantly lower than [^{3}H]flutemetamol (p = 0.1485; df = 6; t-test). [b]The binding capacity of [^{3}H]AZD4694 was not significantly higher than [^{3}H]flutemetamol (p = 0.1437; df = 6; t-test).

The selectivity of AZD4694 binding was in this initial study examined only at high concentration (10 μM) in assays consisting of a panel of 99 enzymes, receptors transporters, and ion channels (MDS Pharma). AZD4694 inhibited at least 50% of radioligand binding to Monoamine oxidase A (82%), phosphodiesterase 4 (73%), Rho-associated coiled-coil containing protein kinase 1 (ROCK1) (64%), adenosine A1 (76%), A2A (93%) and A3 receptors (69%), noradrenaline transporter (50%), and the peripheral benzodiazepine receptor (82%). None of the proteins in the panel were completely inhibited. However, this assay was run at high concentration and calculated from affinity values of AZ4694 toward amyloid fibrils *in vitro*, the predicted selectivity is between 450- and 4500-fold. Taken into account the tracer concentrations, typically < 1 ug total mass injected, used in a clinical PET application the low affinity of AZD4694 toward above mentioned targets is not expected to give any detectable additional binding. The selectivity profile of AZD4694 is very similar to [^{11}C]AZD2184, a radioligand for which no evident secondary binding has been observed *in vivo* (Nyberg *et al.* 2009).

Autoradiography *in vitro*

In vitro autoradiography imaging comparing the binding profile of [^{3}H]AZD4694 with [^{3}H]flutemetamol and [^{3}H]PIB was performed on adjacent 10 μm tissue section from prefrontal cortex from three confirmed AD cases (Fig. 3a). The Aβ plaque pathology was confirmed by immunohistochemistry (IHC) using a mix of two different anti-Aβ antibodies detecting different epitopes of the Aβ peptide (6E10/4G8), this antibody combination was used to monitor total plaque load in Tg2576 mice (Fig. 4a) and human cases (Fig. 4b and c). Immunohistochemistry with 6E10 only has been reported to have poor sensitivity to diffuse plaques (Dickson, 2005). The 6E10/4G8 IHC demonstrated abundant Aβ-plaque load in all three cases, including core plaques, Aβ associated to blood vessels as well as diffuse Aβ deposits.

Binding of 1 nM of [^{3}H]AZD4694 showed a punctuate labeling in tissue sections from all three cases. The binding was most abundant in the superficial layers of the cortex

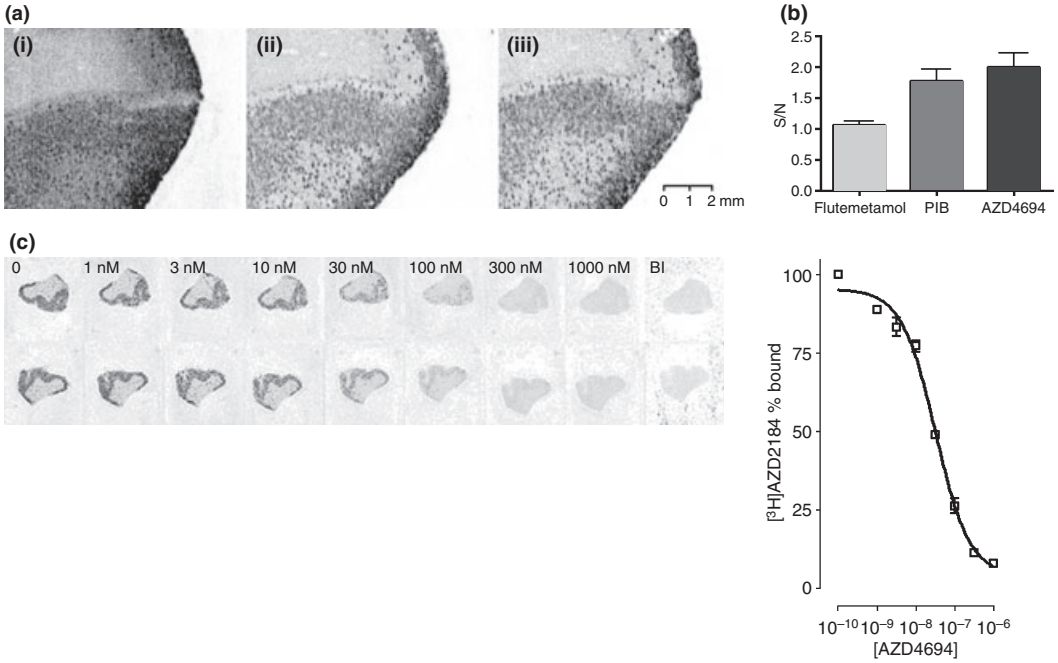

Fig. 3 (a) Comparison of autoradiograms from sections of human Alzheimer's disease (AD) prefrontal cortex incubated with 1 nM of either (i) [^{3}H]flutemetamol, (ii) [^{3}H]PIB, or (iii) [^{3}H]AZD4694. All ligands have similar overall binding profiles labeling Aβ deposits mainly in gray matter. However, note the more defined plaque labeling properties and lower non-specific white matter binding of [^{3}H]AZD4694 compared with [^{3}H]flutemetamol. (b) Bar graphs illustrating the difference in S/N ratio of [^{3}H]flutemetamol, [^{3}H]PIB, or [^{3}H]AZD4694 in human AD prefrontal cortex. The signal-to-noise (S/N) ratio is defined by analysis of total binding in gray matter minus the non-specific binding to subcortical white matter divided by non-specific subcortical white matter binding. Binding intensity was quantified with Fujifilm Multi Gauge V3.0 software. (c) Representative autoradiogram and competition graph derived from the autoradiograms illustrating the displacement of 1 nM [^{3}H]AZD2184 by increasing concentrations of AZD4694 on tissue sections from prefrontal cortex from human AD brain. The graph shows the mean of three data points from plaque-rich grey matter from two tissue sections at each concentration. 1 μM of AZD4694 could fully displace 1 nM [^{3}H]AZD2184 (K_i = 23.1 nM) illustrating that the two ligands are competing for the same binding site.

(gray matter) and more sparse in subcortical white matter. Adjacent sections labeled with [^{3}H]flutemetamol and [^{3}H]PIB corresponded well with the binding profile of [^{3}H]AZD4694 and there was an apparent one-to-one localization between the three ligands and Aβ immunoreactive plaques (Fig. 4b).

To further determine the identity of [^{3}H]AZD4694 binding, emulsion dipped, [^{3}H]AZD4694-treated brain sections from AD cases or Tg2576 mice were compared with Aβ IHC on adjacent sections under light microscope. [^{3}H]AZD4694 and anti-Aβ antibodies labeled identical structures in AD brain tissue, i.e., Aβ plaques and vascular Aβ deposits (Fig. 4c). Blood vessels and the core of Aβ plaques were most intensely labeled whereas diffuse deposits and outer border of core plaques had relatively weaker staining (lower number of silvergrains/area), which could reflect the amount of fibrillar Aβ (Fig. 4d).

Furthermore, AZD4694 could fully displace [^{3}H]AZD2184, which we previously have shown to detect congophilic and non-congophilic Aβ plaques as well as congophilic, Aβ-positive blood vessels (Johnson *et al.* 2009). Although [^{3}H]AZD4694 and [^{3}H]flutemetamol were highly similar in their regional selectivity patterns, the amount of non-specific binding, and the resolution of the plaque signal from the PI derived images differed. Non-specific binding to white matter was about 40% lower for [^{3}H]AZD4694 when compared with [^{3}H]flutemetamol at a ligand concentration of 1 nM.

The relatively lower non-specific binding of [^{3}H]AZD4694 translated into a desired higher S/N ratio for [^{3}H]AZD4694 compared with [^{3}H]flutemetamol but similar to [^{3}H]PIB (Fig. 3b).

CNS exposure

Intravenous cassette dosing was used to compare the *in vivo* pharmacokinetic characteristics of the candidate radioligands. Analysis of brain tissue concentration showed that the compounds quickly entered and rapidly cleared from normal rat brain tissue. AZD4694 had a more rapid washout when compared with flutemetamol (Table 2). The decline in brain exposure between 2 and 30 min was 10× for AZD4694 and 3.6× for flutemetamol with corresponding

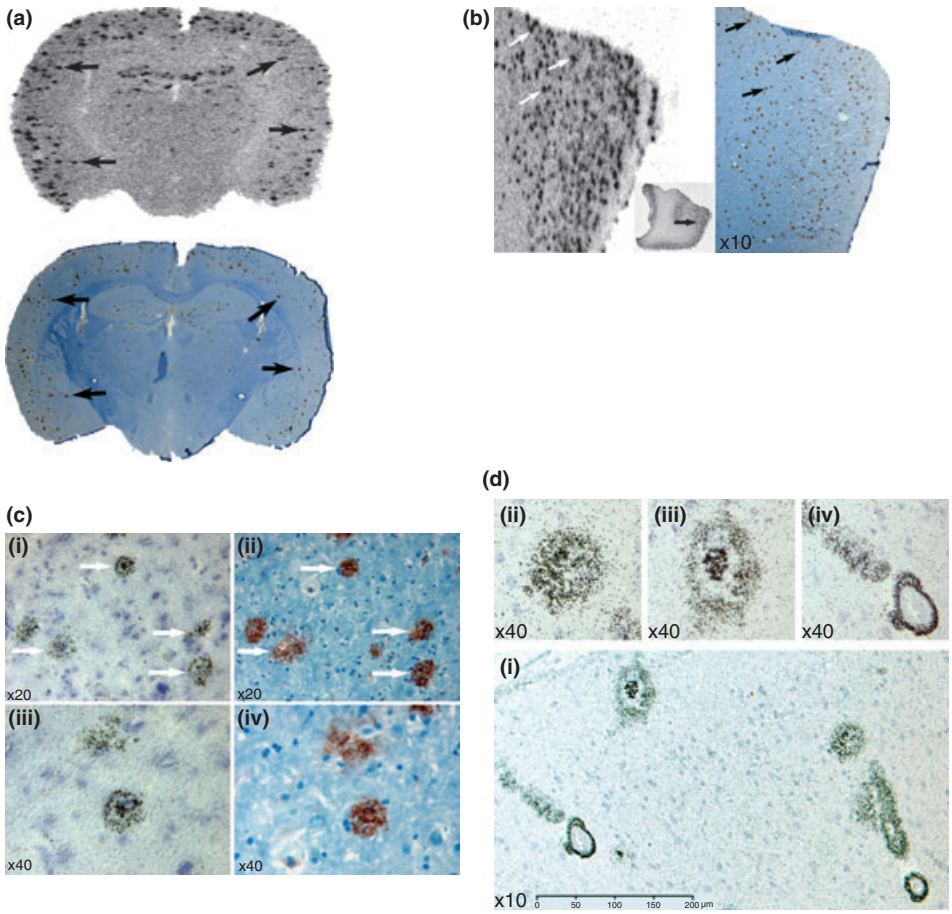

Fig. 4 (a) Images of adjacent representative coronal sections from a Tg2576 mouse showing the autoradiogram of binding of 1 nM of [^{3}H]AZD4694 (top) compared with 6E10/4G8 immunoreactive Aβ deposits (bottom). (b) Images of adjacent representative sections from human Alzheimer's disease (AD) prefrontal cortex showing autoradiogram of binding of 1 nM of [^{3}H]AZD4694 (left) compared to 6E10/4G8 immunoreactive Aβ deposits (right). Insert shows overview of tissue section. (c) Photomicrographs of emulsion dipped developed tissue sections from human AD prefrontal cortex (left) stained with 1 nM [^{3}H]AZD4694. Clusters of dark silver grains indicates the presence of Aβ plaques bound by the ligand. Compared with adjacent sections stained with 6E10/4G8 anti-Aβ antibodies (right). Upper panel 20× magnification lower panel 40× magnification. Matched plaques are marked by arrows, note good correspondence between the two markers. (d) Panel of photomicrographs of emulsion dipped developed tissue sections from human AD prefrontal cortex illustrating different pathological structures stained with 1 nM [^{3}H]AZD4694. (i) 10× magnification overview showing plaques and blood vessels labeled by [^{3}H]AZD4694, arrows indicate structures shown in higher magnification on top. (ii) 40× photomicrograph of plaque with an evenly distributed cluster of silver grains. (iii) 40× photomicrograph of plaque with intensely labeled core surrounded by a weaker labeled halo. (iv) 40× photomicrograph of blood vessel intensely stained by [^{3}H]AZD4694, note the labeled tail of the vessel, probably representing the outer border of the vessel extension.

half-lives of 8.4 and 15.2 min, respectively. At 2 min after drug administration, the percentage of the total administered dose in brain was calculated to be 1.0% for AZD4694 and 2.5% for flutemetamol. In this study, only the concentrations of parent compound were analyzed. While AZD4694 decrease in brain and plasma was comparable (half-lives were 8.4 and 7.5 min, respectively), flutemetamol had a 50% longer half-life in brain than plasma (15.2 and 10.1 min, respectively). The most plausible reason for this is non-specific binding of flutemetamol to brain tissue.

Autoradiography *ex vivo*

To investigate if the imaging properties of [^{3}H]AZD4694 also translates after *in vivo* administration, 150 nmol/kg [^{3}H]AZD4694 and [^{3}H]flutemetamol were injected via the tail vein to 26-months-old Tg2576 mice ($n = 2$) that subsequently were killed 10 min post-injection. [^{3}H]AZD4694 showed notably better binding properties after *in vivo* administration than [^{3}H]flutemetamol. [^{3}H]AZD4694 had a S/N ratio of 1.5 which is higher than for [^{3}H]flutemetamol, having a S/N ratio of 0.6 (Fig. 5b). [^{3}H]AZD4694 also showed a more distinct labeling of

Table 2 Brain exposure of flutemetamol and AZD4694 after intravenous administration in rats

Compound	Dose (μmol/kg)	Brain conc. at 2 min (nM)	Brain conc. at 30 min (nM)	$t_{1/2}$ brain (min)	Fraction in brain at 2 min (%)	Decline in brain exposure 2/30 min
Flutemetamol	0.25	3505	980	15.2	2.5	3.6×
AZD2184	0.25	1550	154	8.4	1.0	10×

plaques than [^{3}H]flutemetamol, which generated an image that was more diffuse with unclear plaque definition, similar to what was observed with *in vitro* autoradiography (Fig. 5a).

To confirm the identity of [^{3}H]AZD4694 binding *in vivo*, autoradiography data were compared with congo red labeling and Aβ IHC in adjacent sections from mouse injected with [^{3}H]AZD4694 (data not shown). [^{3}H]AZD4694 and congo red labeled identical fibrillar plaques and vascular amyloid deposits structures in adjacent 10 μm cortical sections. The [^{3}H]AZD4694, congo red positive amyloid deposits were also immunolabeled by antibodies directed to Aβ (4G8 and 6E10, data not shown).

Autoradiography *ex vivo* time course

To assess the imaging properties of [^{3}H]AZD4694 with time, the kinetics of the specific and non-specific binding in Tg2576 mice were performed. The retention of [^{3}H]AZD4694 in plaque-rich areas and in plaque-free areas at different time points after *in vivo* administration of 150 nmol/kg (i.v) of compound were compared. Autoradiograms of unrinsed sections illustrating [^{3}H]AZD4694 binding in Tg2576 transgenic mouse brain are shown in Fig. 6(a). Quantification of non-specific binding as measured in corpus callosum showed that the non-specific binding peaked at 5 min and declined over time and were barely detectable after 40 min (Fig. 6b). The specific binding of [^{3}H]AZD4694 to amyloid plaques was quantified with an area fraction analysis using the Image J software. Already after 5 min [^{3}H]AZD4694 had entered the brain and labeled amyloid plaques. The plaque associated specifically bound ligand, remained longer than the non-specifically bound non-plaque associated ligand. At 40 min after injection, most of the ligand found in the brain was associated to amyloid-β plaques. However, at the 80 min time point, the specifically bound [^{3}H]AZD4694 had also significantly declined, indicating reversible binding properties. The rapid clearance of radioactivity from plaque-devoid regions and the slow clearance from plaque-rich regions indicates that AZD4694 has a pharmacokinetic profile suitable for PET imaging since a high S/N ratio was obtained early after injection.

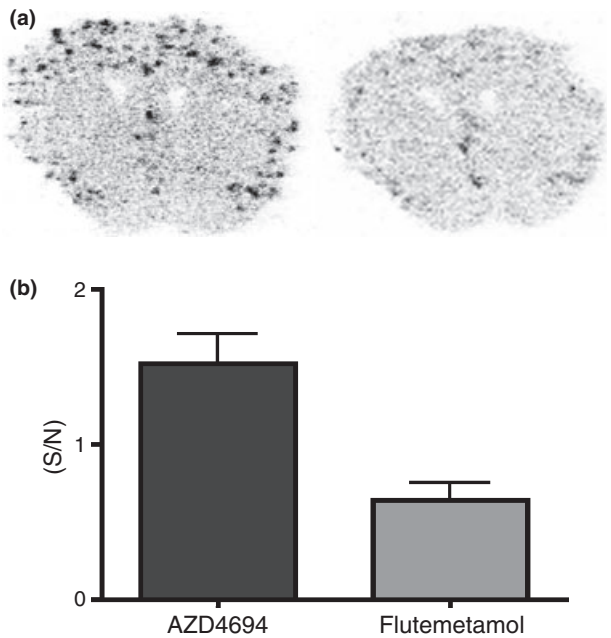

Fig. 5 (a) Comparison of autoradiograms from rinsed sections from Tg2576 mice after *in vivo* (i.v.) administration of 150 nmol/kg of either [^{3}H]AZD4694 (left) or [^{3}H]flutemetamol (right) collected 10 min post-injection. The improved *in vitro* imaging properties of [^{3}H]AZD4694 compared with [^{3}H]flutemetamol translates after *in vivo* administration of ligand. (b) Quantification of signal-to-background (S/N) ratio after *in vivo* administration 150 nmol/kg of [^{3}H]AZD4694 or [^{3}H]flutemetamol with Fuji film Multi Gauge software.

Discussion

The most widely used *in vivo* approach to image cerebral amyloid to date is based on molecular imaging using PET radioligands such as [^{11}C]PIB (Klunk *et al.* 2004; Klunk and Mathis 2008). Although carbon-11 labeled amyloid ligands are promising for diagnostic purposes and to support anti-amyloid clinical trials, the short 20 min radioactive decay half-life of carbon-11 limits their use to PET centers having on-site cyclotron and carbon-11 radiochemistry capability. To increase accessibility and reduce cost at routine use there is a need to develop PET ligands labeled with fluorine-18. The 110 min radioactive decay half-life of this radionuclide allows for centralized production and regional distribution as currently practiced worldwide in the supply of [^{18}F]fluoro-deoxyglucose. There are currently three fluorine-18 labeled Aβ plaque-selective PET radioligands in clinical trials, [^{18}F]flutemetamol, [^{18}F]Florbetaben, and [^{18}F]Florpiramine. Published data on [^{18}F]Flutemetamol and [^{18}F]Florbetaben indicates that both ligands have rather high level of

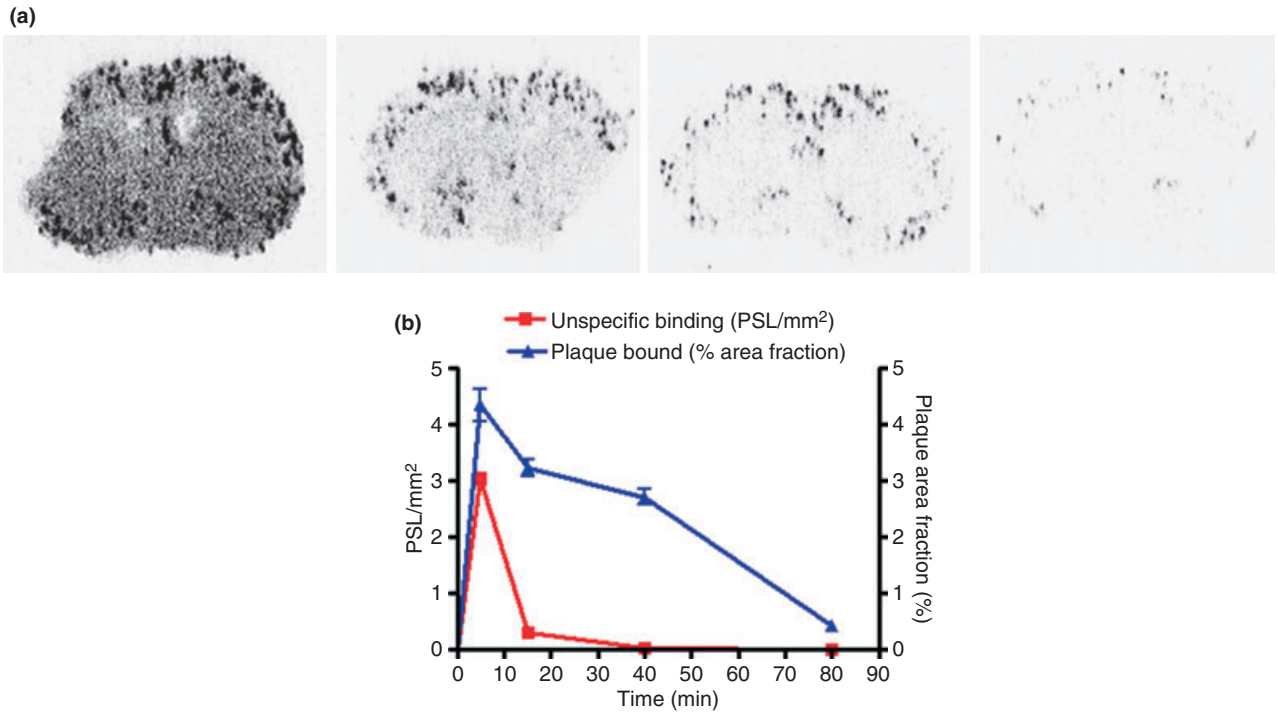

Fig. 6 (a) Autoradiograms of un-rinsed brain sections from Tg2576 at different time points (5, 15, 40, and 80 min) post-injection of 150 nmol/kg (i.v) [^{3}H]AZD4694. (b) Graph illustrating the non-specific binding in corpus callosum (red squares) and the specific plaque associated binding in cortex (blue triangles) over time after *in vivo* administration of 150 nmol/kg [^{3}H]AZD4694. Note the quick appearance and disappearance of the non-plaque-associated radioactivity and the more slow decline of [^{3}H]AZD4694 bound to plaques.

non-specific white matter retention (Mathis *et al.* 2007a; Rowe *et al.* 2008; Nelissen *et al.* 2009). This might be less of a limitation in situations with high cortical insoluble Aβ plaque load. However, the spill over effects of radioactivity from non-specific binding in white matter to adjacent cortical regions may limit their use for accurate mapping of Aβ plaque load in low-density regions and in prodromal phases of AD when insoluble Aβ levels might be low. Thus, there is a need for fluorine-18 labeled Aβ plaque-selective PET tracers with lower non-specific binding to white matter.

The major aim of this study was to develop a selective and sensitive fluorine-18 labeled PET radioligand of cerebral fibrillar Aβ-amyloid with low non-specific binding. Similar to the development of [^{11}C]AZD2184 (Johnson *et al.* 2009; Swahn *et al.* 2010), a screening cascade was adopted to a medicinal chemistry effort aiming at minimizing non-specific binding. Non-specific binding is partly a function of LogP/LogD and besides measuring LogD (Lombardo *et al.* 2001), non-specific binding was approached by cassette dosing experiments in rat where the brain exposure of ligands was compared between 2 and 30 min post-i.v. administration.

From the screening cascade, the radioligand candidate 2-(2-fluoro-6-methylamino-pyridin-3-yl)-benzofuran-5-ol was selected. In the initial characterization, AZD4694 bound with low nanomolar affinity to β-amyloid fibrils *in vitro*. Displacement studies showed that similar to PIB and flutemetamol, AZD4694 fully displaced [^{3}H]AZD2184 binding to β-amyloid fibrils *in vitro*, supporting the view that the site for specific binding is identical for the above mentioned compounds.

We have previously shown that [^{3}H]AZD2184 shares the same binding site as PIB in synthetic Aβ(1–40) fibrils as well as in tissue sections from AD brains (Johnson *et al.* 2009). The frequency of high-affinity binding sites is about 1 site per 600 monomers Aβ(1–40) fibrils. This low frequency and high affinity pattern is similar to what has been published for PIB and AZD2184 (Klunk *et al.* 2004, 2005; Johnson *et al.* 2009) further supporting the view that all test compounds bind to the same site.

High-resolution autoradiography in fresh frozen brain sections in combination with Aβ IHC on adjacent sections confirmed that AZD4694 selectively binds to Aβ fibrils in human postmortem AD brain and in transgenic mouse plaque models. AZD4694 was evaluated side-by-side with flutemetamol and although both ligands have similar high affinity for β-amyloid their level of non-specific binding *in vitro* was different. The lower non-specific binding observed for AZD4694 compared with flutemetamol translates into an improved contrast, which is illustrated in the *in vitro* and *ex vivo* autoradiography images (Figs 3 and 5). The slightly higher ElogD value of flutemetamol (ElogD 3.2) compared

with AZD4694 (ElogD 2.8) could be one explanation for this difference. We have previously shown that a low degree of non-specific binding of [^{3}H]AZD2184 as evaluated using *in vitro* and *ex vivo* autoradiography translates into low levels of non-specific binding of [^{11}C]AZD2184 in cynomolgus monkeys and in man (Johnson *et al.* 2009; Nyberg *et al.* 2009; Andersson *et al.* 2010).

The Aβ plaque binding of [^{3}H]AZD4694 was further examined using *ex vivo* autoradiography in old Tg2576 mice. Taken together, this experiment shows that similar to AZD2184 and PIB, AZD4694 labels amyloid plaques with high specificity in Tg2576 mice after *in vivo* administration. The time course study showed that [^{3}H]AZD4694 labels Aβ plaques in a reversible manner, reaching a peak value between 5 and 15 min at which time S/N is about 1.5. For [^{11}C]AZD2184, reversible binding and rapid establishment of *in vivo* transient equilibrium conditions has been shown to translate in short acquisition times for reliable quantification in human PET-studies (Nyberg *et al.* 2009). This short acquisition time is an advantage for routine clinical use. On the basis of the demonstrated regional time courses and reversibility of [^{3}H]AZD4694 binding demonstrated in this study, [^{18}F]AZD4694 has potential to share the same advantageous kinetic features as [^{11}C]AZD2184 for imaging in AD patients.

In a recent study, it has been shown that PIB may be selective for a pathological human-specific conformation of aggregated Aβ (Rosen *et al.* 2009). Some caution must accordingly be exercised when comparing results from different methods for Aβ plaque load *in vitro.* From a translational perspective, it might be wise to include a validated Aβ plaque-selective PET radioligand when evaluating plaque load *in vitro*. Indeed, AZD4694 as well as AZD2184 detects plaques differently in human AD than in plaque mouse models. In APP/PS1 and Tg2576 mice fibrillar, congo red positive core plaques are detected but not diffuse deposits. In human AD brain, however, both diffuse and core plaques are labeled by thioflavin derived PET ligands at low nM concentrations (Johnson *et al.* 2009). This is in accordance with previously data showing that thioflavin-type PET tracers are non-specific for Aβ insoluble deposits (i.e., diffuse, fibrillar or dense core and vascular plaques) (Lockhart *et al.* 2007). [^{11}C]PIB has been evaluated in over 40 different centers and in 3000 participants around the worlds, including postmortem analysis of AD patients (Ikonomovic *et al.* 2008; Klunk and Mathis 2008). To take advantage of the knowledge already gained in these studies, Klunk and Mathis (2008) has suggested that new fluorine-18 labeled tracers should be compared and evaluated side-by-side with PIB (Klunk and Mathis 2008). Our preclinical data shows that AZD4694 share similar binding profile as PIB and our previously developed radioligand [^{11}C]AZD2184 both *in vitro* and *ex vivo*. The reversible specific binding and low levels of non-specific binding suggests that [^{18}F]AZD4694 has potential for sensitive quantification of Aβ plaques in AD patients.

Acknowledgements

The authors would like to thank the Physiochemical Characterization Team at the Medicinal Chemistry Department for determining ElogD values, NAEJA Pharmaceuticals Inc., Canada for the supply of synthesized compounds and Stefan Elofsson, Anne Svensson, and Maria Nilsson for excellent technical assistance.

References

Aizenstein H. J., Nebes R. D., Saxton J. A. *et al.* (2008) Frequent amyloid deposition without significant cognitive impairment among the elderly. *Arch. Neurol.* **65**, 1509–1517.

Andersson J., Varana K., Cselenyi Z. *et al.* (2010) Radiosynthesis of the candidate β-amyloid radioligand [11C]AZD2184: positron emission tomography examination and metabolite analysis in cynomolgus monkeys. *Synapse* (in press).

Bennett D. A., Schneider J. A., Wilson R. S., Bienias J. L. and Arnold S. E. (2004) Neurofibrillary tangles mediate the association of amyloid load with clinical Alzheimer's disease and level of cognitive function. *Arch. Neurol.* **61**, 378–384.

Braak H. and Braak E. (1991) Neuropathological staging of Alzheimer-related changes. *Acta Neuropathol. (Berl.)* **82**, 239–259.

Dickson D. W. (2005) Required techniques and useful molecular markers in the neuropathologic diagnosis of neurodegenerative diseases. *Acta Neuropathol. (Berl.)* **109**, 14–24.

Fodero-Tavoletti M. T., Rowe C. C., McLean C. A., Leone L., Li Q.-X., Masters C. L., Cappai R. and Villemagne V. L. (2009) Characterization of PIB binding to white matter in Alzheimer's disease and other dementias *J. Nucl. Med.* **50**, 198–204.

Ikonomovic M. D., Klunk W. E., Abrahamson E. E. *et al.* (2008) Post-mortem correlates of in vivo PiB-PET amyloid imaging in a typical case of Alzheimer's disease. *Brain* **131**, 1630–1645.

Johnson A. E., Jeppsson F., Sandell J., Wensbo D., Neelissen J. A., Juréus A., Ström P., Norman H., Farde L. and Svensson S. P. S. (2009) AZD2184: a radioligand for sensitive detection of beta-amyloid deposits. *J. Neurochem.* **108**, 1177–1186.

Klunk W. E. and Mathis C. A. (2008) The future of amyloid-beta imaging: a tale of radionuclides and tracer proliferation *Curr. Opin. Neurol.* **21**, 683–687.

Klunk W. E., Engler H., Nordberg A. *et al.* (2004) Imaging brain amyloid in Alzheimer's disease with Pittsburgh compound-B. *Ann. Neurol.* **55**, 306–319.

Klunk W. E., Lopresti B. J., Ikonomovic M. D. *et al.* (2005) Binding of the positron emission tomography traces Pittsburgh compound-B reflects the amount of amyloid–β in Alzheimer's disease brain but nou in transgenic mouse brain. *J. Neurosci.* **25**, 10598–10606.

Knopman D. S., Parisi J. E., Salviati A. *et al.* (2003) Neuropathology of cognitively normal elderly. *J. Neuropathol. Exp. Neurol.* **62**, 1087–1095.

Lockhart A., Lamb J. R., Osredkar T., Sue L. I., Joyce J. N., Ye L., Libri V., Leppert D. and Beach T. G. (2007) PIB is a non-specific imaging marker of amyloid-beta (Abeta) peptide-related cerebral amyloidosis. *Brain* **130**, 2607–2615.

Lombardo F., Shalaeva M. Y., Tupper K. A. and Gao F. (2001) ELogD(oct): a tool for lipophilicity determination in drug discovery. 2. Basic and neutral compounds. *J. Med. Chem.* **44**, 2490–2497.

Mathis C. A., Lopresti B. J., Mason N., Price J. C., Flatt N., Bi W., Ziolko S., DeKosky S. and Klunk W. E. (2007a) Comparison of the amyloid imaging agents [F18]3′-FPIB and [C-11]PIB in Alzheimer's disease and control subjects. *J. Nucl. Med.* **48**(Suppl. 2), 56.

Mathis C. A., Lopresti B. J. and Klunk W. E. (2007b) Impact of amyloid imaging on drug development in Alzheimer's disease. *Nucl. Med. Biol.* **34**, 809–822.

Morris J. C., Roe C. M., Grant E. A., Head D., Storandt M., Goate A. M., Fagan A. M., Holtzman D. M. and Mintun M. A. (2009) Pittsburgh Compound B imaging and prediction of pregression from cognitive normality to symptomatic Alzheimer Disease. *Arch. Neurol.* **66**, 1469–1475.

Necula M., Kayed R., Milton S. and Glabe C. G. (2007) Small molecule inhibitors of aggregation indicate that amyloid β oligomerization and fibrillization pathways are independent and distinct. *J. Biol. Chem.* **282**, 10311–10324.

Nelissen N., Van Laere K., Thurfjell L., Owenius R., Vandenbulcke M., Koole M., Bormans G., Brooks D. J. and Vandenberghe R. (2009) Phase 1 study of the Pittsburgh compound B derivative 18F-flutemetamol in healthy volunteers and patients with probable Alzheimer disease. *J. Nucl. Med.* **50**, 1251–1259.

Nelson P. T., Braak H. and Markesbery W. R. (2009) Neuropathology and cognitive impairment in Alzheimer disease: a complex but coherent relationship. *J. Neuropathol. Exp. Neurol.* **68**, 1–14.

Nilsson M. R. (2004) Techniques to study amyloid fibril formation in vitro. *Methods* **34**, 151–160.

Nyberg S., Jörnhagen M. E., Cselényi Z. *et al.* (2009) Detection of amyloid in Alzheimer's disease with positron emission tomogragphy using [^{11}C]AZD2184. *Eur. J. Nucl. Med. Mol. Imaging* **36**, 1859–1863.

Pike K. E., Savage S., Villemange V. L., Ng S., Moss S. A., Maruff P., Mathis C. A., Klunk W. E., Masters C. L. and Rowe C. C. (2007) β-amyloid imaging and memory in non-demented individuals: evidence for preclinical Alzheimer's disease. *Brain* **130**, 2837–2844.

Price J. L., Davis P. B., Morris J. C. and White D. L. (1991) The distribution of tangles, plaques and related immunohistochemical markers in healthy aging and Alzheimer's disease. *Neurobiol. Aging* **12**, 295–312.

Price J. L., McKeel Jr D. W., Buckles V. D. *et al.* (2009) Neuropathology of nondemented aging: presumptive evidence for preclinical Alzheimer disease. *Neurbiol. Aging* **30**, 1026–1036.

Rinne J. O., Brooks D. J., Rossor M. N. *et al.* (2010) (11)C-PiB PET assessment of change in fibrillar amyloid-beta load in patients with Alzheimer's disease treated with bapineuzumab: a phase 2, double-blind, placebo-controlled, ascending-dose study. *Lancet Neurol.* **9**, 363–372.

Rosen R. F., Walker L. C. and LeVine H. (2009) PIB binding in aged primate brain: enrichment of high-affinity sites in humans with Alzheimer's disease. *Neurobiol. Aging*. doi: 10.1016/jneurobiolaging.2009.02.011.

Rowe C. C., Ackerman U., Browne W. *et al.* (2008) Imaging of amyloid β in Alzheimer's disease with ^{18}F-BAY94-9172, a novel PET tracer: proof of mechanism. *Neurology* **7**, 129–135.

Sperling R. A., LaViolette P. S., O'Keefe K. *et al.* (2009) Amyloid deposition is associated with impaired default network function in older persons without dementia. *Neuron* **63**, 178–188.

Swahn B. M., Wensbo D., Sandell J. *et al.* (2010) Synthesis and evaluation of 2-pyridylbenzothiazole, 2-pyridyl-benzoxazole and 2-pyridylbenzofuran derivatives as 11C-PET imaging agents for β-amyloid plaques. *Bioorg. Med. Chem. Lett.* **20**, 1976–1980.

Villemagne V. L., Pike K. E., Darby D. *et al.* (2008) Abeta deposits in older non-demented individuals with cognitive decline are indicative of preclinical Alzheimer's disease. *Neuropsychologia* **46**, 1688–1697.

Yang F., Lim G. P., Begum A. N. *et al.* (2005) Curcumin inhibits formation of amyloid β oligomers and fibrils, binds plaques, and reduces amyloid in vivo. *J. Biol. Chem.* **280**, 5892–5901.

